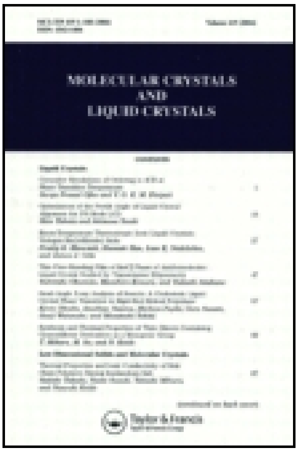

Molecular Crystals and Liquid Crystals Incorporating Nonlinear Optics
Publication details, including instructions for authors and subscription information:
http://www.tandfonline.com/loi/gmcl17

BEDT-TTF Salts with Square-Planar Gold(III) Complex Anions: β-$(ET)_2AuCl_4$ and $(ET)_2Au(CN)_2Cl_2$

Urs Geiser [a] , Benjamin A. Anderson [a] , Ann Murray [a] , Catherine M. Pipan [a] , Carol A. Rohl [a] , Bradley A. Vogt [a] , Hau H. Wang [a] , Jack M. Williams [a] , Dae Bok Kang [b] & Myung-Hwan Whangbo [b]

[a] Chemistry and Materials Science Divisions, Argonne National Laboratory, Argonne, IL, 60439, USA

[b] Department of Chemistry, North Carolina State University, Raleigh, NC, 27695, USA

To cite this article: Urs Geiser , Benjamin A. Anderson , Ann Murray , Catherine M. Pipan , Carol A. Rohl , Bradley A. Vogt , Hau H. Wang , Jack M. Williams , Dae Bok Kang & Myung-Hwan Whangbo (1990): BEDT-TTF Salts with Square-Planar Gold(III) Complex Anions: β-$(ET)_2AuCl_4$ and $(ET)_2Au(CN)_2Cl_2$, Molecular Crystals and Liquid Crystals Incorporating Nonlinear Optics, 181:1, 105-116

To link to this article: http://dx.doi.org/10.1080/00268949008035996

Mol. Cryst. Liq. Cryst., 1990, vol. 181, pp. 105–116
Reprints available directly from the publisher
Photocopying permitted by license only

Printed in the United States of America

BEDT-TTF SALTS WITH SQUARE-PLANAR GOLD(III) COMPLEX ANIONS: β-$(ET)_2AuCl_4$ AND $(ET)_2Au(CN)_2Cl_2$

URS GEISER, BENJAMIN A. ANDERSON, ANN MURRAY, CATHERINE M. PIPAN, CAROL A. ROHL, BRADLEY A. VOGT, HAU H. WANG, AND JACK M. WILLIAMS
Chemistry and Materials Science Divisions, Argonne National Laboratory, Argonne, IL 60439 (USA)

DAE BOK KANG AND MYUNG-HWAN WHANGBO
Department of Chemistry, North Carolina State University, Raleigh, NC 27695 (USA)

Abstract We report the synthesis, crystal structures, and band electronic structures of the first 2:1 salts of the organic donor radical cation bis(ethylenedithio)tetrathiafulvalene (BEDT-TTF or ET) with square-planar anions, i. e., β-$(ET)_2AuCl_4$ (**1**) and $(ET)_2Au(CN)_2Cl_2$ (**2**). The crystal and the band electronic structures of **1** are related to the β-phase superconductors, β-$(ET)_2X$ ($X = I_3$, IBr_2, AuI_2). However, β-$(ET)_2AuCl_4$ undergoes a destructive phase transition after prolonged cooling to 126 K and is non-superconducting. Temperature-dependent ESR measurements of **2** indicate a very broad metal-to-insulator phase transition between 250 and 300 K. The band electronic structure of **2** indicates 1-d metallic behavior at room temperature with a well nested open Fermi surface. Crystal parameters: β-$(ET)_2AuCl_4$: triclinic, $P\bar{1}$, a = 6.590(2) Å, b = 8.561(2) Å, c = 18.319(5)°, α = 93.19(2)°, β = 105.52(2)°, γ = 119.47(2)°, V_c = 845.1(3) Å^3, Z = 1. $(ET)_2Au(CN)_2Cl_2$: monoclinic, $P2/c$, a = 17.726(8) Å, b = 6.690(4) Å, c = 15.284(10) Å, β = 108.19(5)°, V_c = 1722(2) Å^3, Z = 2.

INTRODUCTION

Bis(ethylenedithio)tetrathiafulvalene (BEDT-TTF or ET) and its analogs crystallize with a number of linear, monovalent anions, X^-, to form superconducting, 2:1 salts $(ET)_2X$.[1] These include β-$(ET)_2I_3$ (superconducting transition temperature, T_c = 1.4 K at ambient pressure;[2] T_c = 8.0 K in 0.5 kbar pressure[3] or after special heat treatment),[4] β-$(ET)_2IBr_2$ (T_c = 2.8 K),[5] β-$(ET)_2AuI_2$ (T_c = 4.8 K),[6] κ-$(ET)_2I_3$,[7] κ-$(MDT\text{-}TTF)_2AuI_2$ (T_c = 4.5 K),[8] and $(DMET)_2X$ ($X^- = Au(CN)_2^-$, $AuBr_2^-$, I_3^-, and IBr_2^-, $T_c \leq 1.5$ K).[9] Most planar anions have yielded ET-salts of stoichiometry different from 2:1, with the exception of $(ET)_2C(CN)_3$,[10] which contains a trigonal-planar tricyanomethanide anion. To date, none of the ET salts with planar anions are superconducting. As part of our ongoing research on the influence of the anion shapes on the donor-layer packing patterns, and thus the electronic properties of organic donor salts, we have recently prepared the first 2:1 salts of ET with square-planar anions, $(ET)_2AuCl_4$ and $(ET)_2Au(CN)_2Cl_2$, whose crystal structures, physical properties, and band electronic structures we describe here.

EXPERIMENTAL

Both, β-$(ET)_2AuCl_4$ (**1**) and $(ET)_2Au(CN)_2Cl_2$ (**2**), were synthesized by electrocrystallization on Pt electrodes. In the preparation of **1**, a solution of 24 mM $(PPN)AuCl_4$ [PPN^+ is bis(triphenylphosphine)iminium cation, $\{(C_6H_5)_3P\}_2N^+$; prepared from reagent grade $HAuCl_4 \cdot xH_2O$ and (PPN)Cl in ethanol, recrystallized from CH_2Cl_2:diethylether] and 1.66 mM ET (Strem Chemical Co.) in dry THF were employed with a current density of 1 μAcm^{-2}. The conditions in the synthesis of **2** were 1.66 mM ET and 8 mM $[(n\text{-}C_4H_9)_4N]Au(CN)_2Cl_2$, also in dry THF at a current density of 0.1 μAcm^{-2}.

Crystals of compound **1** are small lustrous blocks with faces parallel to the unit cell axes. In addition to these well-formed crystals, large amounts of micro-

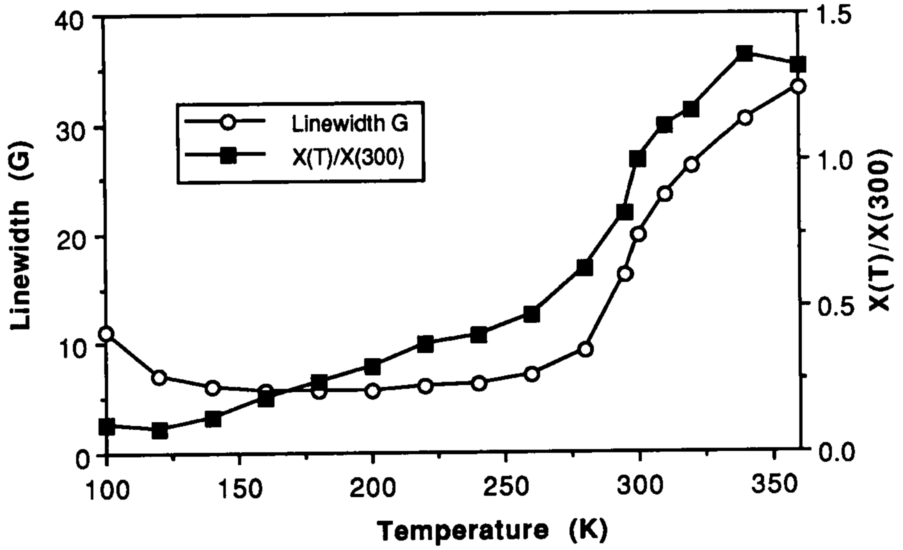

FIGURE 1 ESR line width and relative spin susceptibility in $(ET)_2Au(CN)_2Cl_2$, indicating a broad phase transition centered around 300 K.

crystalline material are usually formed. The room temperature ESR line width, ΔH_{pp}, is 12–15 G, which is somewhat smaller than the corresponding value $\Delta H_{pp} \approx 20$ G for the superconductors β-$(ET)_2X$ ($X^- = I_3^-$, AuI_2^-, and IBr_2^-).[11] None of the crystals were large enough for the electrical conductivity to be measured by the four-probe technique. Crystals of **2** are black lustrous square-like plates (the plate normal is a^*). The electrical conductivity, measured below room temperature, is that of a semiconductor, but log(R) vs. $1/T$ does not follow a straight line, indicating a variable gap. However, an average activation energy, $E_a \approx 0.18$ eV was estimated from the slope $\partial[\log(R)]/\partial(1/T)$ between 140 and 170 K. The room temperature value of the electrical conductivity was measured, $\sigma_{300} \approx 0.05\ (\Omega\text{cm})^{-1}$.

The ESR behavior of **2** is more complicated: Spectra were measured in the temperature range 100–360 K, and the results are shown in Fig. 1. Both, line width and spin susceptibility (estimated by double integration of the first-derivative ESR spectrum), show a strong drop from the highest temperature measured down to about 250 K, where the changes in both parameters become smaller. At the lowest temperatures, the line width starts to increase again. Very similar behavior has been found in the compounds $(ET)_2QF_6$ (Q = As, Sb),[12] which also are structurally similar to $(ET)_2Au(CN)_2Cl_2$ (vide infra).

X-ray single crystal data collection parameters are summarized in Table I. For both structures, the data were corrected for Lorentz, polarization, and absorption effects (Gaussian integration). The structure of **1** was solved by use of the heavy

TABLE I Crystal (room temperature), data collection , and refinement parameters for β-$(ET)_2AuCl_4$ and $(ET)_2Au(CN)_2Cl_2$.

	β-$(C_{10}H_8S_8)_2AuCl_4$	$(C_{10}H_8S_8)_2Au(CN)_2Cl_2$
a, b, c (Å)	6.590(2), 8.561(2), 18.319(5)	17.726(8), 6.690(4), 15.284(10)
α, β, γ (°)	93.19(2), 105.52(2), 119.47(2)	90, 108.19(5), 90
V_c (Å^3), Z	845.1(3), 1	1722(2), 2
Space group	triclinic, $P\bar{1}$	monoclinic, $P2/c$
2θ-range (°), no. refl.	4 – 50, 3390	4 – 48, 4995
Min. hkl; max. hkl	0, –9, –21; 7, 8, 20	–20, –2, –2; 19, 7, 17
Scan type, range, speed	$\theta/2\theta$, 2.1–2.4°, 1.5–12 °min^{-1}	$\theta/2\theta$, 2.3–2.6°, 2–10 °min^{-1}
Crystal size (mm^3)	0.10×0.15×0.18	0.03×0.20×0.27
μ (cm^{-1}), T_{min}, T_{max}	56, 0.32, 0.59	53.7, 0.399, 0.851
R_{ave}, wR_{ave}, unique allowed	0.010, 0.013, 2996	0.053, 0.032, 2729
Min. $F_o/\sigma(F_o)$, reflns used	2.0, 2895	4.0, 1960
No. variables	187	188
$R(F_o)$, $wR(F_o)$, $G.O.F.$	0.031, 0.037, 2.46	0.057, 0.054, 2.19

atom method (Au atom at unit cell origin) and by subsequent Fourier calculations. For **2**, the structure was solved by direct methods yielding all Au, Cl, and S atoms, and eight of the ET-carbon atoms and completed by Fourier calculations. The ethylene end groups of **2** were modelled by two conformations for each of the 6-membered rings. Isotropic thermal factors were constrained to be equal for C-atoms 7A, 7B, 8A, and 8B, and similarly for 9A, 9B, 10A, and 10B. Analogously, the occupational factors of carbon atoms 7A and 8A (63 %), and 9A and 10A (58 %) were constrained to be equal. Furthermore, the occupational parameters of the B-conformation atoms (C7B–C10B) were required to complement those of the A-conformation. No hydrogen atoms were included in either structure analysis. All other atoms were varied with anisotropic parameters in the full-matrix least-squares refinement. No evidence for extinction effects was found in either data crystal. Final positional parameters for β-$(ET)_2AuCl_4$ and $(ET)_2Au(CN)_2Cl_2$ are given in Tables II and III, respectively. Anisotropic thermal parameters and structure factors are available from the authors upon request.

TABLE II Atomic coordinates and equivalent isotropic thermal parameters for β-$(ET)_2AuCl_4$.

Atom	x	y	z	$U_{eq}\times10^4$
Au	0.0000	0.0000	0.0000	432(1)
Cl1	0.3617(3)	0.2784(2)	0.03353(9)	591(6)
Cl2	–0.1508(4)	0.1208(2)	0.06775(12)	1008(10)
S1	0.9099(3)	0.1953(2)	0.49491(8)	554(6)
S2	0.5189(3)	0.2804(2)	0.46007(8)	652(7)
S3	0.9124(2)	0.2009(2)	0.67238(7)	468(6)
S4	0.5227(3)	0.2880(2)	0.63504(7)	523(6)
S5	0.9408(3)	0.1803(3)	0.33872(9)	821(9)
S6	0.4770(3)	0.2881(2)	0.29686(8)	749(8)
S7	0.9940(3)	0.2472(2)	0.84111(7)	600(7)
S8	0.5213(3)	0.3457(3)	0.79349(8)	732(8)
C1	0.7132(9)	0.2369(7)	0.5282(3)	433(22)
C2	0.7157(9)	0.2398(7)	0.6027(3)	396(21)
C3	0.8013(10)	0.2185(7)	0.4005(3)	468(23)
C4	0.6243(10)	0.2580(7)	0.3843(3)	448(22)
C5	0.8274(9)	0.2500(7)	0.7496(3)	380(20)
C6	0.6506(9)	0.2891(7)	0.7325(3)	407(21)
C7	0.8276(22)	0.2481(19)	0.2569(5)	2078(89)
C8	0.6140(17)	0.2434(15)	0.2326(4)	1357(58)
C9	0.9350(11)	0.3827(8)	0.9020(3)	558(26)
C10	0.6662(12)	0.3128(8)	0.8845(3)	647(28)

TABLE III Atomic coordinates and equivalent isotropic thermal parameters for $(ET)_2Au(CN)_2Cl_2$.

Atom	x	y	z	$U_{eq}\times10^4$
Au	0.0000	0.5000	0.5000	435(3)
Cl	0.0158(2)	0.5756(6)	0.6490(3)	678(17)
N	0.0892(8)	0.098(2)	0.5716(10)	758(66)
C11	0.0563(8)	0.239(2)	0.5456(10)	472(60)
S1	0.4774(2)	0.4215(5)	0.1154(3)	526(15)
S2	0.4368(2)	−0.0006(7)	0.1234(2)	529(13)
S3	0.6516(2)	0.2902(6)	0.1063(3)	487(15)
S4	0.6141(2)	−0.1270(6)	0.1309(3)	523(17)
S5	0.3271(3)	0.5748(6)	0.1299(5)	1109(29)
S6	0.2737(2)	0.0722(5)	0.1268(3)	533(15)
S7	0.8203(2)	0.2201(6)	0.1259(3)	560(16)
S8	0.7746(2)	−0.2804(6)	0.1583(3)	706(19)
C1	0.5079(7)	0.174(2)	0.1200(9)	377(51)
C2	0.5809(7)	0.116(2)	0.1184(10)	382(54)
C3	0.3844(8)	0.364(2)	0.1256(10)	459(58)
C4	0.3641(7)	0.171(2)	0.1267(9)	384(52)
C5	0.7290(8)	0.116(2)	0.1240(10)	336(54)
C6	0.7111(9)	−0.075(2)	0.1346(11)	436(59)
C7A	0.2293(13)	0.463(4)	0.087(2)	461(42)
C7B	0.240(2)	0.474(7)	0.139(3)	461
C8A	0.2201(14)	0.290(4)	0.149(2)	461
C8B	0.209(3)	0.282(7)	0.104(3)	461
C9A	0.8786(13)	−0.007(5)	0.125(2)	466(40)
C9B	0.889(2)	0.014(7)	0.186(2)	466
C10A	0.8727(15)	−0.159(4)	0.200(2)	466
C10B	0.865(2)	−0.179(6)	0.143(3)	466

CRYSTAL STRUCTURE DESCRIPTIONS

β-$(ET)_2AuCl_4$

The ET donor molecule and the atomic labeling are shown in Figure 2. The ET molecule is located on a general position in the crystal structure, whereas the gold atom of the nearly square-planar $AuCl_4^-$ anion occupies a center of inversion. For the $AuCl_4^-$ anion, the difference in the two Au–Cl bond lengths (0.015 Å) is statistically significant, but the deviation of the Cl–Au–Cl angle from 90° is not. The crystal packing consists of ET donor layers in the *ab*-plane, separated by the layers of the $AuCl_4^-$ anions along the *c*-direction. The plane of each anion is not parallel to the *ab*-plane but inclined to the donor network with a 35.1° dihedral angle. Therefore the

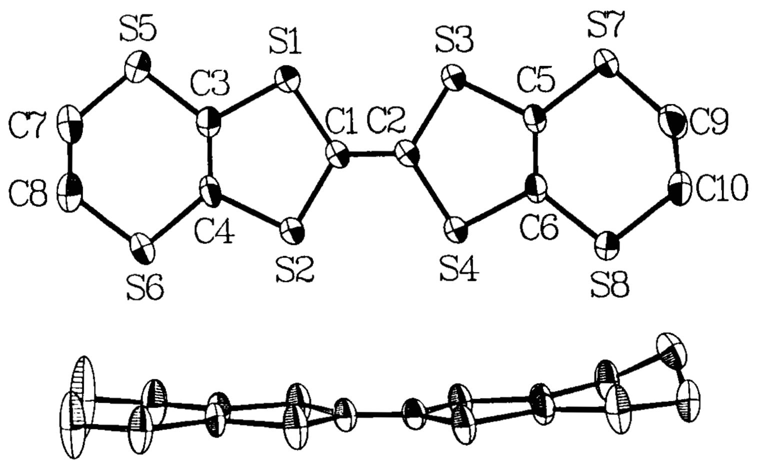

FIGURE 2 ET molecule (hydrogen atoms excluded) of β-$(ET)_2AuCl_4$ with atomic labeling. The temperature factor ellipsoids are drawn at the 50% level at room temperature. The same atomic labeling was used in $(ET)_2Au(CN)_2Cl_2$.

donor sheets are more separated in β-$(ET)_2AuCl_4$ than in the β-$(ET)_2X$ salts with linear-triatomic anions X^-. This larger separation is reflected in an increase of the length of *c* by approximately 3 Å over that of the other β-structures.

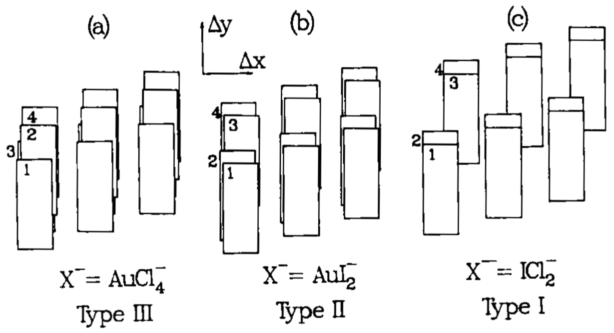

FIGURE 3 Schematic representation of the ET molecule donor radical network in three β-like $(ET)_2X$ structures: (a) β-$(ET)_2AuCl_4$; (b) β-$(ET)_2AuI_2$; (c) β'-$(ET)_2ICl_2$. The rectangles are formed by the "outer" sulfur atoms, S5–S8, and the projection is perpendicular to the ET molecular plane in each case.

Shown schematically in Figure 3 are the packing arrangements of the donor networks in the various β-like $(ET)_2X$ structural types, where each rectangle represents an ET molecule viewed perpendicular to the π-framework of the ET molecule. The stacking pattern of $\beta\text{-}(ET)_2AuCl_4$ is similar to, but not identical to that of the superconducting β-phases. The structural differences in the three phases, types I-III, may best be described in terms of the relative displacements Δx and Δy, between nearest-neighbor ET molecules along the stack. Δx is the displacement along the short axis of the donor molecule, whereas Δy is that along the long molecular axis. The values of Δx and Δy described below are calculated from the coordinates of the centers of the C1–C2 bonds in nearest-neighbor ET molecules.

All β-like structure types possess two donor molecules per repeat distance along the stack. In the triclinic space group $P\bar{1}$, this amounts to two nonequivalent pair-wise interactions and thus to two sets of Δx- and Δy-values for each structure type. The Δx displacements in the structure types III (–0.21 and +0.39 Å) and II (–0.16 and +0.38 Å, calculated for $\beta\text{-}(ET)_2AuI_2$ at room temperature) are essentially identical and, except for the sign change, show very little alternation along the stack. On the other hand, the type I salts exhibit strongly alternating Δx values (e.g., Δx = 0.06 and 2.14 Å for the ICl_2^- salt). However, the signs of the Δx- displacements remain the same in the type I salts, unlike in types II and III. The principal difference between the latter lies in the relative displacements along the y-direction: in the type III structure, Δy changes sign from –1.60 to +3.44 Å whereas the corresponding values in II are +1.28 and +3.54 Å, thus having the same sign. Equal signs are also seen in the Δy values of type I salts, but again with larger alternation of the values, viz. 1.34 and 5.77 Å. In summary, the type I salts are regarded as strongly dimerized along the stacking direction, whereas the stacking is more uniform in the type II and III salts.

Upon cooling for several hours at 126 K, crystals of $\beta\text{-}(ET)_2AuCl_4$ shattered suddenly into many pieces of microcrystalline material. Even though it was not possible to collect a complete intensity data set before the phase transition occurred, a set of unit cell parameters of **1** at 126 K, where it is metastable, could be obtained: a = 6.565(2) Å, b = 8.483(2), c = 18.289(6) Å, α = 93.62(2)°, β = 105.59(3)°, γ = 119.66(2)°, V_c = 828.7(4) Å^3. Axial rotation photographs around the crystal axes revealed no significant change from the corresponding room temperature photos, except for the lattice contraction. Thus, it is unlikely that the phase transition is of electronic origin. More likely, it is due to steric crowding, leading to unfavorably short contacts between ethylene group hydrogen atoms and anion chlorine atoms, and thus to a build-up of internal strain which is ultimately relieved in a phase transition to a more stable phase. The transition likely involves large atomic and molecular motions and is therefore destructive to macroscopic crystals.

$(ET)_2Au(CN)_2Cl_2$

The same atomic labeling scheme was used as in the structure of β-$(ET)_2AuCl_4$ (Figure 2). Each unit cell (shown in Figure 4) contains one layer (*bc*-plane) comprising one stack of donor molecules, with a repeating pattern of 4 molecules along the stacking axis, *c*. Two types of interactions are found along the stack: pairs of ET molecules are arranged around centers of inversion in a "face-to-face" mode, i. e., parallel to each other and with the connecting line between molecule centers approximately perpendicular to the molecular plane (angle between connecting vector and plane normal: 28°). The other intrastack interaction type is grouped around a 2-fold rotations axis perpendicular to the stack. Here, the planes of the molecules are also parallel to each other (3° dihedral angle), but the long axes of the molecules (i. e., the directions of the the central C=C bonds) are twisted considerably with respect to each other (33°). Furthermore, the molecules are slipped along the long axis by approximately 1.6 Å ≈ $(x_{C1}+x_{C2}-1.0)a$. This packing arrangement within the ET donor molecular layer is very similar to that found[12] in $(ET)_2SbF_6$ and implied in $(ET)_2AsF_6$. However, the space group found in the latter two compounds, *I*2/*c* in the

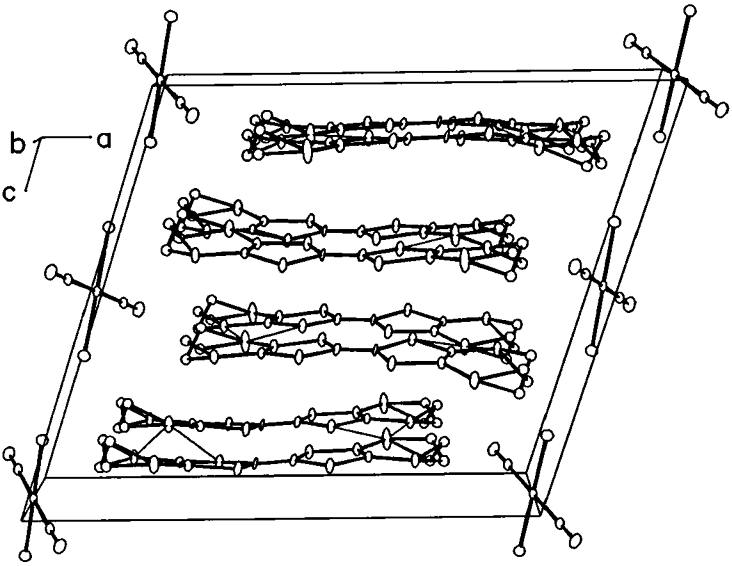

FIGURE 4 Projection of the crystal structure of $(ET)_2Au(CN)_2Cl_2$ along the *b*-axis. Thin lines represent S···S contacts shorter than 3.6 Å.

setting used in ref. 12, requires two layers per unit cell, thus the compounds are not isostructural.

The presence of a phase transition near room temperature became known after the structural analysis was completed. It is assumed that the structure described here represents the high-temperature phase. Low temperature diffraction experiments will be carried out in the future.

BAND ELECTRONIC STRUCTURES

The band electronic structures of β-$(ET)_2AuCl_4$ and $(ET)_2Au(CN)_2Cl_2$ were examined by performing tight-binding band calculations[13] based on the extended Hückel method.[14] We used double-zeta Slater type orbitals,[15] and calculated $H_{\mu\nu}$ values by employing a modified Wolfsberg-Helmholtz formula[16] (for details, see ref. 13).

β-$(ET)_2AuCl_4$

Shown in Figure 5 (left) are the two highest occupied bands calculated for the room temperature crystal structure of β-$(ET)_2AuCl_4$. These two bands originate mainly

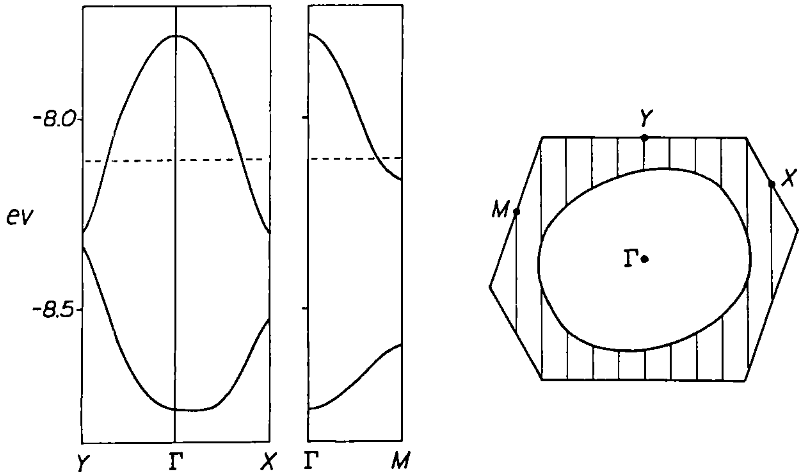

FIGURE 5 (Left) Dispersion relations for the two highest occupied bands of β-$(ET)_2AuCl_4$. The dashed line refers to the Fermi level, and Γ, X, Y, and M represent wave vector points (0, 0), ($a^*/2$, 0), (0, $b^*/2$), and ($-a^*/2$, $b^*/2$), respectively, of the first Brillouin zone within the a^*b^*-plane. (Right) The Fermi surface associated with the half-filled band of β-$(ET)_2AuCl_4$, where the wave vectors of the shaded and unshaded regions lead to occupied and unoccupied levels, respectively.

from the HOMO of each ET molecule, and with the formal oxidation of $(ET)_2^+$ per unit cell the upper band is half-filled. This band is equally dispersive along the stacking and the interstack directions, so that in a low-spin band-filling scheme the resulting Fermi surface is closed as shown in Figure 5 (right). Consequently, β-$(ET)_2AuCl_4$ is expected to be a two-dimensional metal. Experimental confirmation of this prediction must await the availability of larger crystals.

$(ET)_2Au(CN)_2Cl_2$

The dispersion relations of the two highest occupied bands of $(ET)_2Au(CN)_2Cl_2$ are shown in Fig. 6, where the upper band is half-filled due to the formal oxidation state $(ET)_2^+$. Also shown in Fig. 6 is the Fermi surface associated with this band. It is open along $\Gamma \rightarrow Z$ (i.e., the interstack direction), so that this compound is expected to be a one-dimensional metal along the stacking direction, *c*. The observed semiconducting properties of $(ET)_2Au(CN)_2Cl_2$ below the phase transition near room temperature are likely related to the nesting of its Fermi surface (which is based on the high-temperature crystal structure) along the direction $\mathbf{q} = \mathbf{c}^* + 0.5\ \mathbf{b}^*$. Low temperature x-ray diffraction experiments should reveal the presence of superlattice reflections from a doubling of the *b*-axis if the Fermi surface nesting causes a charge density wave transition.

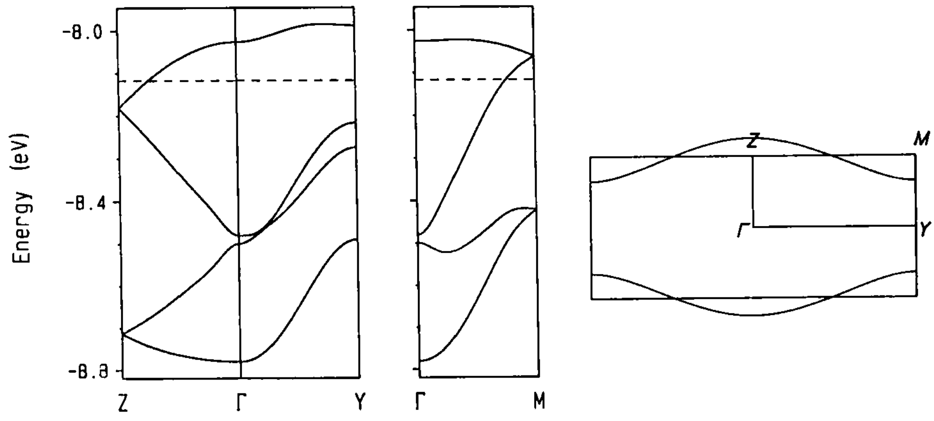

FIGURE 6 (Left) Dispersion relations for the highest occupied bands of $(ET)_2Au(CN)_2Cl_2$. The dashed line indicates the Fermi level, and Γ, Y, Z, and M represent wave vector points (0, 0), ($b^*/2$, 0), (0, $c^*/2$), and ($b^*/2$, $c^*/2$), respectively, of the first Brillouin zone within the b^*c^*-plane. (Right) The Fermi surface associated with the half-filled band of $(ET)_2Au(CN)_2Cl_2$.

CONCLUSIONS

The crystal structures, selected physical properties, and the band electronic structures of the new charge transfer salts β-$(ET)_2AuCl_4$ and $(ET)_2Au(CN)_2Cl_2$ have been reported. These salts are the first 2:1 salts of ET with *square-planar* counter-ions. The first salt is structurally related to the superconducting β-phases containing linear triatomic anions. A novel destructive low temperature phase transition, likely unrelated to the electronic structure, is found upon cooling crystals of the compound for prolonged periods of time. The crystal structure, semiconducting properties and temperature dependence of the ESR parameters of $(ET)_2Au(CN)_2Cl_2$ are very similar to those found in $(ET)_2SbF_6$ and similar materials. They all undergo a broad phase transition to an insulating state near or slightly below room temperature. In the case of the PF_6 salt, a doubling of the *b*-axis, due to Fermi surface nesting, has been previously observed.[17] Low-temperature diffraction experiments on $(ET)_2Au(CN)_2Cl_2$ are yet to be carried out, but the similarity of the other properties, especially the Fermi surface nesting, suggests an analogous doubling of the unit cell may occur.

Acknowledgements:

Work at Argonne National Laboratory and North Carolina State University is sponsored by the U. S. Department of Energy, Office of Basic Energy Sciences, Division of Materials Sciences, under Contract W-31-109-ENG-38 and Grant DE-FG05-86ER45259, respectively. B. A. A., A. M., C. M. P., C. A. R., and B. A. V. are student undergraduate research participants, sponsored by the Argonne Division of Educational Programs, from Wittenberg University, Springfield (OH), Humboldt State University, Arcata (CA), Immaculata College, Immaculata (PA), Rice University, Houston (TX), and University of Minnesota, Morris (MN), respectively.

REFERENCES

1. J. M. Williams, H. H. Wang, T. J. Emge, U. Geiser, M. A. Beno, P. C. W. Leung, K. D. Carlson, R. J. Thorn, A. J. Schultz, M.-H. Whangbo, *Prog. Inorg. Chem.*, *35*, 51 (1987).
2. É. B. Yagubskiĭ, I. F. Shchegolev, V. N. Laukhin, P. A. Kononovich, M. W. Karatsovnik, A. V. Zvarykina, L. I. Buravov, *JETP Lett.*, *39*, 12 (1984).
3. (a) V. N. Laukhin, E. É. Kostyuchenko, Yu. V. Sushko, I. F. Shchegolev, É. B. Yagubskiĭ, *JETP Lett.*, *41*, 81 (1985). (b) K. Murata, M. Tokumoto, H. Anzai,

H. Bando, G. Saito, K. Kajimura, T. Ishiguro, *J. Phys. Soc. Jpn.*, *54*, 1236 (1985).

4. (a) G. O. Baram, L. I. Buravov, L. S. Degtyarev, M. É. Kozlov, V. N. Laukhin, E. É. Laukhina, V. G. Onishchenko, K. I. Pokhdonya, M. K. Sheĭnkman, R. P. Shibaeva, É. B. Yagubskiĭ, *JETP Lett.*, *44*, 376 (1986). (b) D. Schweitzer, P. Bele, H. Brunner, E. Gogu, U. Haeberlen, I. Hennig, T. Klutz, R. Swietlik, H. J. Keller, *Z. Phys. B* (*Cond. Matt.*), *67*, 489 (1987).
5. J. M. Williams, H. H. Wang, M. A. Beno, T. J. Emge, L. M. Sowa, P. T. Copps, F. Behroozi, L. N. Hall, K. D. Carlson, G. W. Crabtree, *Inorg. Chem.*, *23*, 3839 (1984)
6. H. H. Wang, M. A. Beno, U. Geiser, M. A. Firestone, K. S. Webb, L. Nuñez, G. W. Crabtree, K. D. Carlson, J. M. Williams, L. J. Azevedo, J. F. Kwak, J. E. Schirber, *Inorg. Chem.*, *24*, 2465 (1985).
7. A. Kobayashi, R. Kato, H. Kobayashi, S. Moriyama, Y. Nishio, K. Kajita, W. Sasaki, *Chem. Lett.*, 459 (1987).
8. (a) G. C. Papavassiliou, G. A. Mousdis, J. S. Zambounis, A. Terzis, A. Hountas, B. Hilti, C. W. Mayer, J. Pfeiffer, *Synth. Met.*, *27*, B379 (1988). (b) A. M. Kini, M. A. Beno, D. Son, H. H. Wang, K. D. Carlson, L. C. Porter, U. Welp, B. A. Vogt, J. M. Williams, D. Jung, M. Evain, M.-H. Whangbo, D. L. Overmyer, J. E. Schirber, *Solid State Commun.*, *69*, 503 (1989). MDT-TTF = methylenedithio-tetrathiafulvalene.
9. K. Kikuchi, K. Murata, Y. Honda, T. Namiki, K. Saito, H. Anzai, K. Kobayashi, T. Ishiguro, I. Ikemoto, *J. Phys. Soc. Jpn.*, *56*, 4241 (1987). DMET = 4,5-dimethyl-9,10-ethylenedithio-1,3-diselena-6,8-dithiafulvalene.
10. M. A. Beno, H. H. Wang, L. Soderholm, K. D. Carlson, L. N. Hall, L. Nuñez, H. Rummens, B. Anderson, J. A. Schlueter, J. M. Williams, M.-H. Whangbo, M. Evain, *Inorg. Chem.*, *28*, 150 (1989).
11. P. C. W. Leung, M. A. Beno, T. J. Emge, H. H. Wang, M. K. Bowman, M. A. Firestone, L. M. Sowa, J. M. Williams, *Mol. Cryst. Liq. Cryst.*, *125*, 113 (1985).
12. R. Laversanne, J. Amiell, P. Delhaes, D. Chasseau, C. Hauw, *Solid State Commun.*, *52*, 177 (1984).
13. M.-H. Whangbo, J. M. Williams, P. C. W. Leung, M. A. Beno, T. J. Emge, H. H. Wang, K. D. Carlson, G. W. Crabtree, *J. Am. Chem. Soc.*, *107*, 5815 (1985).
14. R. Hoffmann, *J. Chem. Phys.*, *39*, 1397 (1963).
15. E. Clementi, C. Roetti, *At. Data Nucl. Data Tables*, *14*, 177 (1974).
16. J. H. Ammeter, H.-B. Bürgi, J. C. Thibeault, R. Hoffmann, *J. Am. Chem. Soc.*, *100*, 3686 (1978).
17. T. Mori, A. Kobayashi, Y. Sasaki, R. Kato, H. Kobayashi, *Solid State Commun.*, *53*, 627 (1985).